Analytic perturbation theory for screened Coulomb potentials: Relativistic case*

James McEnnan,† David J. Botto, and R. H. Pratt
Department of Physics, University of Pittsburgh, Pittsburgh, Pennsylvania 15260

Doina Bunaciu and Viorica Florescu
Theoretical Physics Department, Faculty of Physics, University of Bucharest and National Center of Physics, Bucharest-Magurele, P. O. Box 5211, Romania

(Received 7 July 1977)

Analytic expressions for relativistic screened Coulomb radial wave functions, including bound-state energy eigenvalues as well as bound and continuum wave-function shapes and normalizations, are given explicitly as series in $\lambda \simeq \alpha Z^{1/3}$. The method employed is a direct generalization of an approach previously used for the nonrelativistic case. The analytic expansions which we obtain are compared with exact numerical solutions of the Dirac equation for relativistic Hartree-Slater potentials. Low-, intermediate-, and high-Z cases are considered for a wide range of energies and angular momenta. In general, excellent agreement is found for both inner bound states and for relativistic continuum states.

I. INTRODUCTION

We have recently considered an analytic perturbation theory for the construction of nonrelativistic screened Coulomb wave functions[1] which is based on an expansion of the potential in the interior of the atom of the form

$$V(r) = (-a/r)[1 + V_1\lambda r + V_2(\lambda r)^2 + V_3(\lambda r)^3 + \cdots] , \tag{1}$$

where $a = \alpha Z$ and $\lambda \equiv 1.13\alpha Z^{1/3}$ is a small parameter characterizing the screening. (α is the fine-structure constant and Z the nuclear charge.) Both bound and continuum states are obtained. Bound-state energy eigenvalues and wave functions are expressed as series in λ with simple analytic coefficients. For inner shells these wave functions are in good agreement with exact numerical results throughout the interior of the atom. Since this includes all of the region in which the wave function is large, bound-state normalizations for these cases are also obtained as series in λ. Continuum states may be obtained simply by analytic continuation from the bound-state case using the substitution $\eta \to -i\nu = -ia/p_c$. This requires the introduction of an additional (Coulomb) energy parameter which is shifted by a definite amount from the physical kinetic energy associated with the continuum wave function. By considering also the irregular (Jost) solution we obtain an expansion for the continuum normalization. In a subsequent paper[2] this theory was extended to include the possibility of arbitrary energy shift.

These nonrelativistic screened wave functions have been applied to the calculation of photoeffect cross sections in nonrelativistic dipole approximation.[3] Excellent results are obtained in comparison with exact numerical evaluations in the same screened potential. More recently the procedure has been extended to a systematic study of photoeffect from atomic ions,[4] to the nonrelativistic calculation of internal-conversion coefficients[5] and to the screening corrections to radiative electron capture.[6] It is clear, however, that further progress in these areas requires an extension of our theory to the relativistic case.[7]

In the following we present explicit results for solutions of the Dirac equation for realistic screened Coulomb potentials which can be represented in the form (1). The method employed is a direct extension of that employed previously and a detailed exposition of the theory can be found in Refs. (1)–(3). The modifications of the theory which are necessary for the relativistic case as well as our final analytic expressions for both bound and continuum wave functions are given in Secs. II and III. In Sec. IV we compare our analytic results with exact numerical evaluations. In general, we find very good agreement comparable to that obtained in the nonrelativistic case.

II. BOUND STATES

The Dirac equation for a central potential can be written in the form

$$[-i\vec{\alpha}\cdot\nabla + \beta - (E - V)]\psi = 0 , \tag{2}$$

where $\psi = \begin{pmatrix}\phi\\ \chi\end{pmatrix}$, with ϕ and χ two-component spinors, and

$$\vec{\alpha} = \begin{pmatrix}0 & \vec{\sigma}\\ \vec{\sigma} & 0\end{pmatrix}, \quad \beta = \begin{pmatrix}I & 0\\ 0 & -I\end{pmatrix}.$$

We use natural units, $\hbar = c = m_e = 1$, so that distances are measured in electron Compton wavelengths and energies in units of the electron rest-mass energy. $V(r)$ is the screened potential and

E is the energy of the (bound) electron. The regular solutions of this equation which are simultaneous eigenfunctions of H, J^2, J_z and parity can be written in the form

$$\Phi_{E\kappa m}(\vec{r}) = \frac{1}{r}\begin{pmatrix} if_{E\kappa}(r)\Omega_{\kappa m}(\hat{r}) \\ -g_{E\kappa}(r)\Omega_{-\kappa m}(\hat{r}) \end{pmatrix}, \tag{3}$$

where the angular functions $\Omega_{\kappa m}$ are simultaneous eigenfunctions of J^2, L^2, S^2, and J_z. κ is defined by

$$(1+\vec{\sigma}\cdot\vec{L})\Omega_{\kappa m} = \kappa\Omega_{\kappa m} , \tag{4}$$

so that

$$\kappa = \mp(j+\tfrac{1}{2}) = \begin{cases} -(l+1), & j = l+\frac{1}{2} \\ l, & j = l-\frac{1}{2} \end{cases} . \tag{5}$$

Substituting (3) into (2) we obtain the following coupled ordinary differential equations for the radial functions $f(r)$ and $g(r)$,

$$\begin{aligned} &\frac{df}{dr} + \frac{\kappa f}{r} - \left(E_c + 1 + \frac{a}{r}\right)g = (\delta E - \delta V)g , \\ &\frac{dg}{dr} - \frac{\kappa g}{r} + \left(E_c - 1 + \frac{a}{r}\right)f = -(\delta E - \delta V)f , \end{aligned} \tag{6}$$

where $V_c = -a/r$ and E_c is the point-Coulomb binding energy and $\delta E = E - E_c$, $\delta V = V - V_c$.

Defining reduced radial functions $u(r)$ and $v(r)$ such that $f(r) = Nr^{\gamma}e^{-p_c r}u(r)$, $g(r) = Nr^{\gamma}e^{-p_c r}v(r)$ and making a change of variable $x = 2p_c r$, where $\gamma^2 = \kappa^2 - a^2$ and $p_c^2 = 1 - E_c^2$ (N is a normalization constant and will be discussed later), we find the following equations

$$\begin{aligned} &\left(\frac{d}{dx} - \frac{1}{2} + \frac{\gamma+\kappa}{x}\right)u - \left(\frac{E_c+1}{2p_c} + \frac{a}{x}\right)v \\ &\qquad = \frac{1}{2p_c}(\delta E - \delta V)v , \\ &\left(\frac{d}{dx} - \frac{1}{2} + \frac{\gamma-\kappa}{x}\right)v + \left(\frac{E_c-1}{2p_c} + \frac{a}{x}\right)u \\ &\qquad = \frac{-1}{2p_c}(\delta E - \delta V)u . \end{aligned} \tag{7}$$

Finally, we set

$$\begin{pmatrix} u \\ v \end{pmatrix} = A\begin{pmatrix} F_1 \\ F_2 \end{pmatrix} ,$$

where the matrix A is given by

$$A = \frac{1}{\sqrt{2}}\begin{pmatrix} (1+E_c)^{1/2} & (1+E_c)^{1/2} \\ (1-E_c)^{1/2} & -(1-E_c)^{1/2} \end{pmatrix}. \tag{8}$$

$F_1(x)$ and $F_2(x)$ then satisfy the euqations

$$\begin{aligned} &\left(\frac{d}{dx} - 1 + \frac{\gamma+\eta}{x}\right)F_1 + \frac{\kappa+\eta'}{x}F_2 \\ &\qquad = \frac{-1}{2p_c^2}(\delta E - \delta V)(E_c F_1 + F_2) , \end{aligned} \tag{9a}$$

$$\begin{aligned} &\frac{\kappa-\eta'}{x}F_1 + \left(\frac{d}{dx} + \frac{\gamma-\eta}{x}\right)F_2 \\ &\qquad = \frac{1}{2p_c^2}(\delta E - \delta V)(F_1 + E_c F_2) , \end{aligned} \tag{9b}$$

where $\eta = aE_c/p_c$, $\eta' = a/p_c = (\eta^2 + a^2)^{1/2}$.

In order to solve these equations (9) we first rewrite Eq. (9b) in the form

$$\begin{aligned} F_1(x) = \frac{x}{\kappa-\eta'}\Bigg\{ &-\left(\frac{d}{dx} + \frac{\gamma-n}{x}\right)F_2(x) + \frac{1}{2p_c^2} \\ &\times (\delta E - \delta V)[F_1(x) + E_c F_2(x)]\Bigg\} . \end{aligned} \tag{10}$$

We then substitute the right-hand side of Eq. (10) into the left-hand side of Eq. (9a) whenever $F_1(x)$ appears, obtaining

$$\begin{aligned} &-x\left[\frac{d^2}{dx^2} + \left(-1 + \frac{2\gamma+1}{x}\right)\frac{d}{dx} - \frac{\gamma-\eta}{x}\right]F_2(x) \\ &\quad = \mathfrak{D}_{\eta,\gamma}F_2(x) \\ &\quad = -\frac{\kappa-\eta'}{2p_c^2}(\delta E - \delta V)[E_c F_1(x) + F_2(x)] - \frac{x}{2p_c^2}\left(\frac{d}{dx} - 1 + \frac{\gamma+\eta+1}{x}\right)(\delta E - \delta V)[F_1(x) + E_c F_2(x)] . \end{aligned} \tag{11}$$

These equations, (10) and (11), are the basic equations which we have to solve. They are the relativistic analog of Eq. (4) of Ref. 1. In the bound-state case the boundary conditions on $F_1(x)$ and $F_2(x)$ are that the wave function defined by them be square integrable and that the difference between the screened and point-Coulomb wave functions vanish at the origin. (See the discussion

in Ref. 1 and references therein).

Following the procedure of Ref. 1 we expand the solutions of Eqs. (10) and (11) as series in λ of the form[8]

$$F_1(x) = F_1^c(x) + \lambda^2 A_2(x) + \lambda^3 A_3(x) + \cdots ,$$
$$F_2(x) = F_2^c(x) + \lambda^2 B_2(x) + \lambda^3 B_3(x) + \cdots , \tag{12}$$

where $F_1^c(x)$ and $F_2^c(x)$ are the point-Coulomb solutions. Explicitly,

$$F_1^c(x) = (\gamma - \eta)\left(\frac{\eta+\gamma}{\eta'-\kappa}\right)^{1/2} M(\gamma-\eta+1, 2\gamma+1, x)$$
$$= (\gamma-\eta)e^{-\xi} M(\gamma-\eta+1, 2\gamma+1, x) , \tag{13}$$
$$F_2^c(x) = (\gamma+\eta)\left(\frac{\eta-\gamma}{\eta'+\kappa}\right)^{1/2} M(\gamma-\eta, 2\gamma+1, x)$$
$$= (\gamma+\eta)e^{\xi} M(\gamma-\eta, 2\gamma+1, x) ,$$

where $M(a,b,Z)$ is a regular confluent hypergeometric function (CHF) and for bound states, $\eta - \gamma = k = n - |\kappa| = 0,1,2,\ldots$. The boundary conditions require that the coefficients $A_n(x)$ and $B_n(x)$ defining the solutions (12) satisfy the conditions $A_n(0) = B_n(0) = 0$.

We also expand the bound-state energy eigenvalue as a series in λ,

$$E = E_c + \lambda E_1 + \lambda^2 E_2 + \lambda^3 E_3 + \cdots , \tag{14}$$

where E_c, the point-Coulomb binding energy for the state described by the quantum numbers n, κ, is given by

$$E_c = [1 + a^2/(n - |\kappa| + \gamma)^2]^{-1/2} . \tag{15}$$

As in the nonrelativistic case, the requirement of square integrability determines the coefficients E_n.

Finally, employing an expansion of the potential (1) we can obtain analytic expressions for the coefficients $A_n(x)$ and $B_n(x)$ by expanding the right-hand sides of Eqs. (10) and (11) in terms of contiguous CHF according to the relations

$$xM(a,b,x) = aM(a+1,b,x) + (b-2a)M(a,b,x) + (a-b)M(a-1,b,x) ,$$
$$x\left(\frac{d}{dx} - 1\right) M(a,b,x) = (a-b)[M(a,b,x) - M(a-1,b,x)] , \tag{16}$$
$$x\frac{d}{dx} M(a,b,x) = a[M(a+1,b,x) - M(a,b,x)] ,$$

and using the fact that

$$\mathfrak{D}_{\eta,\gamma} M(\gamma-\eta-s, 2\gamma+1, x) = sM(\gamma-\eta-s, 2\gamma+1, x) . \tag{17}$$

Although the algebra is considerably more involved in the relativistic case, the essential features are the same as outlined in Ref. 1. We find, then, that $A_n(x)$ and $B_n(x)$ have the form

$$A_n(x) = \sum_{s=-n}^{n} \alpha_s^n(p_c,\kappa) M(\gamma-\eta+1-s, 2\gamma+1, x) ,$$
$$B_n(x) = \sum_{s=-n}^{n} \beta_s^n(p_c,\kappa) M(\gamma-\eta-s, 2\gamma+1, x) , \tag{18}$$

with

$$\beta_s^n(p_c,\kappa) = \alpha_{-s}^n(-p_c,\kappa) . \tag{19}$$

(We note that $p_c \to -p_c$ implies $\eta \to -\eta$, $\eta' \to -\eta'$, and $\xi \to -\xi$.) Explicit results for these coefficients α_s^n for $n = 2,3$ are given in Table I. We note that in the bound-state case $\alpha_s^n = 0$ unless $\gamma - \eta + 1 - s$ = integer ≤ 0 and $\beta_s^n = 0$ unless $\gamma - \eta - s$ = integer ≤ 0. Hence, the relativistic bound-state functions defined by (12) and (18) will be polynomials to any finite order in λ. At the same time, the bound-state energy eigenvalue, to third-order in λ, is found to be equal to

$$E = E_c - V_1\lambda a + \tfrac{1}{2}\lambda^2 V_2(E_c\kappa^2 + \kappa - 3\eta\eta')$$
$$+ (a\lambda^3 V_3/2p_c^2)[(2E_c^2+1)\kappa^2 + 3E_c\kappa - 4\eta^2 - \eta'^2 - 1] . \tag{20}$$

This analytic expansion of the bound-state wave functions gives a good representation of the exact screened Dirac wave function in the interior region (cf. Figs. 1–4).

Since the wave functions defined by (12) and (18) are square integrable, the determination of the normalization constant N is straightforward. We require

$$\int_0^\infty [f^2(r) + g^2(r)]\, dr = 1 = (2p_c)^{-2\gamma-1} \int_0^\infty x^{2\gamma} e^{-x} [F_1^2(x) + F_2^2(x) + 2E_c F_1(x) F_2(x)]\, dx , \tag{21}$$

which implies

$$N = N_c\{1 - \lambda^2(2\eta')^{-1}[\beta_0^2 e^{\xi} - \alpha_0^2 e^{-\xi} + E_c(\alpha_{+1}^2 e^{\xi} - \beta_{-1}^2 e^{-\xi})] - \lambda^3(2\eta')^{-1}[\beta_0^3 e^{\xi} - \alpha_0^3 e^{-\xi} + E_c(\alpha_{+1}^3 e^{\xi} - \beta_{-1}^3 e^{-\xi})]\}$$
$$= N_c(1 - \lambda^2\gamma_2 - \lambda^3\gamma_3 + \cdots) , \tag{22}$$

TABLE I. Coefficients $\alpha_s^n(p_c,\kappa)$ which appear in our expansion of the screening corrections to the relativistic wave function, Eq. (18).

s	$\frac{\alpha_s^2(p_c,\kappa)}{V_2/4p_c^2}$	$\frac{\alpha_s^3(p_c,\kappa)}{aV_3/8p_c^4}$
−3		$-\frac{1}{3}(\gamma-\eta)(\gamma-\eta+1)(\gamma-\eta+2)(\gamma-\eta+3)e^{-\zeta}E_c$
−2	$-\frac{1}{2}\eta(\gamma-\eta)(\gamma-\eta+1)(\gamma-\eta+2)e^{-\zeta}$	$-\frac{1}{2}(\gamma-\eta)(\gamma-\eta+1)(\gamma-\eta+2)e^{-\zeta}[2\eta'+E_c(4\eta-6)]$
−1	$-(\gamma-\eta)(\gamma-\eta+1)e^{-\zeta}[2\eta'^2+E_c(E_c\kappa^2+\kappa)-\eta(\eta+2)]$	$-(\gamma-\eta)(\gamma-\eta+1)e^{-\zeta}\{E_c[(4E_c^2-1)\kappa^2+6E_c\kappa-4\eta^2-10\eta+4]$ $-3\kappa-5\eta'+9\eta\eta'\}$
+1	$(\gamma+\eta)e^{\zeta}\{[E_c(\kappa+\eta')+1][E_c\kappa^2+\kappa-\eta'(\eta-1)]$ $-\eta'(\gamma+\eta+1)(\gamma-\eta-1)-\eta'(\gamma-\eta)e^{-2\zeta}[\kappa+\eta'+E_c]\}$	$(\gamma+\eta)e^{\zeta}\{[E_c(\kappa+\eta')+1][(4E_c^2+2)\kappa^2+6E_c\kappa-8\eta^2$ $-2\eta'^2-2-(\gamma+\eta+1)(\gamma-\eta-1)+(2\eta+1)^2-(\gamma^2-\eta^2)]$ $-(\gamma-\eta-1)(\gamma+\eta+1)[4(\eta+1)+E_c(\kappa+\eta')]$ $-4\eta(\gamma-\eta)e^{-2\zeta}[E_c+\kappa+\eta']\}$
+2	$-\frac{1}{2}\eta'(\gamma+\eta)(\gamma+\eta+1)e^{\zeta}[E_c(\kappa+\eta')+2]$	$\frac{1}{2}(\gamma+\eta)(\gamma+\eta+1)e^{\zeta}\{(\gamma-\eta-2)(\gamma+\eta+2)-4(\eta+1)[E_c(\kappa+\eta'+2]$ $+(\gamma-\eta)e^{-2\zeta}[2E_c+\kappa+\eta']\}$
+3		$\frac{1}{3}(\gamma+\eta)(\gamma+\eta+1)(\gamma+\eta+2)e^{\zeta}[E_c(\kappa+\eta')+3]$
0	$\alpha_0^2(p_c,\kappa)=-\sum_{s=-2}^{2}{}'\alpha_s^2(p_c,\kappa)=-(\alpha_{-2}^2+\alpha_{-1}^2+\alpha_{+1}^2+\alpha_{+2}^2)$	$\alpha_0^3(p_c,\kappa)=-\sum_{s=-3}^{3}{}'\alpha_s^3(p_c,\kappa)=-(\alpha_{-3}^3+\alpha_{-2}^3+\alpha_{-1}^3+\alpha_{+1}^3+\alpha_{+2}^3+\alpha_{+3}^3)$

where N_c is the point-Coulomb normalization

$$N_c=(2p_c)^{\gamma+1/2}\ \frac{1}{\Gamma(2\gamma+1)}\left(\frac{\Gamma(\eta+\gamma)}{2\eta'\Gamma(\eta-\gamma+1)}\right)^{1/2}. \qquad (23)$$

Although the general expressions for the wave function, etc. are quite complicated in the relativistic case, for the ground state ($n=1, \kappa=-1$) considerable simplification results. We find

$$F_1(x)=\tfrac{1}{2}\gamma^{1/2}x[\Lambda_2+\Lambda_3(\gamma+1+\tfrac{1}{2}x)],$$
$$F_2(x)=2\gamma^{1/2}\{1-\tfrac{1}{4}\Lambda_2 x(2\gamma^2+\gamma-2-\tfrac{1}{2}\gamma x)$$
$$-\tfrac{1}{4}\Lambda_3 x[(\gamma+1)(2\gamma^2+\gamma-2)$$
$$+4x-\tfrac{4}{3}\gamma x^2]\}, \qquad (24)$$

where $\Lambda_n=V_n(\lambda/a)^n$ and $\gamma=(1-a^2)^{1/2}$. The ground-

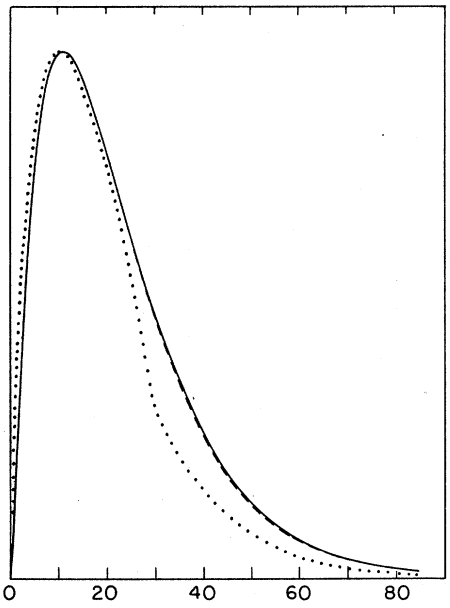

FIG. 1. Upper component $f_{Ek}(r)$ (unnormalized) for the $1S_{1/2}$ state of aluminum ($Z=13$). The unbroken line is the numerical shape obtained for the KS potential, while the dashed curve gives the analytic result. The dotted line is the point-Coulomb shape for the same state. Distances are in electron-Compton wavelengths.

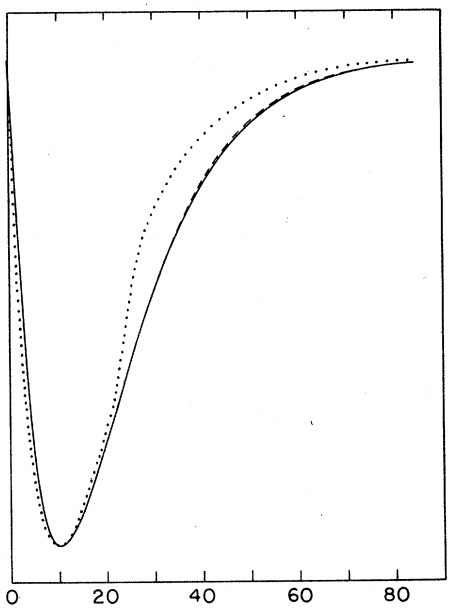

FIG. 2. Lower component $g_{Ek}(r)$ (unnormalized) for the $1S_{1/2}$ state of Al. Otherwise the same as Fig. 1.

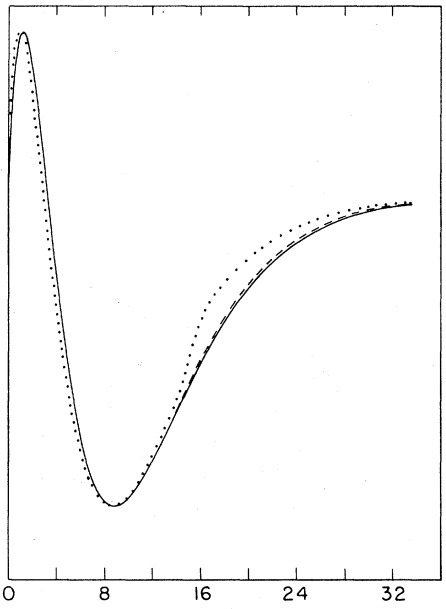

FIG. 3. Upper component (unnormalized) for the $2S_{1/2}$ state of tungsten ($Z=74$) assuming a Yukawa potential $V(r)=-(a/r)e^{-\lambda r}$. λ^{-1} is the Thomas-Fermi radius. The unbroken line gives the exact numerical shape, while the dashed line gives the analytic result. The dotted line is the point-Coulomb shape for the same state. Distances are in electron-Compton wavelengths.

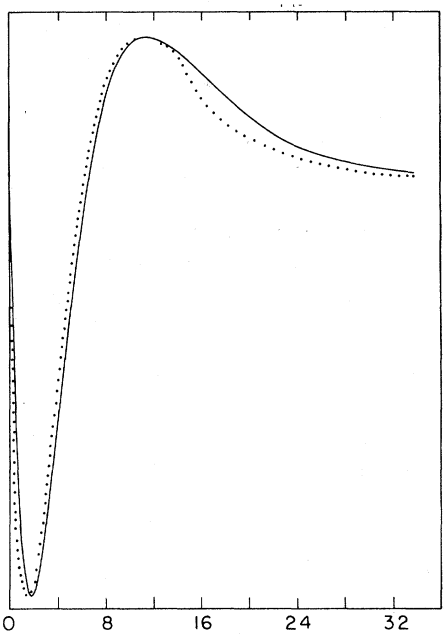

FIG. 4. Lower component (unnormalized) for the $2S_{1/2}$ state of W assuming a Yukawa potential. Otherwise the same as Fig. 3.

state binding energy is given by

$$E=a^2[\gamma/a^2-\Lambda_1-\tfrac{1}{2}\Lambda_2(2\gamma+1) -\tfrac{1}{2}\Lambda_3(\gamma+1)(2\gamma+1)]\,, \tag{25}$$

and the normalization constant is just

$$N=\frac{1}{2\gamma^{1/2}}\frac{(2a)^{\gamma+1/2}}{[\Gamma(2\gamma+1)]^{1/2}} \times[1+\tfrac{1}{4}\Lambda_2(\gamma+1)(2\gamma+1)(\gamma-2) +\tfrac{1}{12}\Lambda_3(\gamma+1)(2\gamma+1)(4\gamma^2-6\gamma-9)]\,. \tag{26}$$

In the nonrelativistic limit, dropping terms of order a^2, these results (24)–(26) as well as our general expression for screened Dirac wave functions reduced to the nonrelativistic wave functions derived previously. This assures, as is the case for the potentials we consider, that as Z decreases the relativistic potential coefficients V_n approach the corresponding nonrelativistic V_n.

III. CONTINUUM STATES

A. Regular solution

For the solutions to the screened Dirac equation in the continuum case, we will follow the the procedure of Ref. (1). Thus, the regular solution is obtained from the bound-state solution by analytic continuation. The extension to arbitrary energy shift (cf. Ref. 2) is discussed briefly in the Appendix. As before, the normalization is obtained from the irregular (Jost) solution.

In the continuum case, the radial wave functions satisfy

$$\frac{df}{dr}+\frac{\kappa f}{r}-\left(E_c+1+\frac{a}{r}\right)g=(\delta E-\delta V)g\,, \qquad \frac{dg}{dr}-\frac{\kappa g}{r}+\left(E_c-1+\frac{a}{r}\right)f=-(\delta E-\delta V)f\,, \tag{27}$$

where now $E\geq 1$ and E_c, the Coulomb energy, is a parameter which will be considered later. We define $f(r)=N\gamma^{\gamma}e^{-ik_c r}u(r)$, $g(r)=N\gamma^{\gamma}e^{-ik_c r}v(r)$ and make a change of variable $x=2ik_c r$. N is again a normalization constant and $k_c^2=E_c^2-1$. We find

$$\left(\frac{d}{dx}-\frac{1}{2}+\frac{\gamma+\kappa}{x}\right)u-\left(\frac{E_c+1}{2ik_c}+\frac{a}{x}\right)v =\frac{1}{2ik_c}(\delta E-\delta V)v\,,$$

$$\left(\frac{d}{dx}-\frac{1}{2}+\frac{\gamma-\kappa}{x}\right)v+\left(\frac{E_c-1}{2ik_c}+\frac{a}{x}\right)u =\frac{-1}{2ik_c}(\delta E-\delta V)u\,. \tag{28}$$

Finally, we write

$$\begin{pmatrix}u\\v\end{pmatrix}=A\begin{pmatrix}F_1\\F_2\end{pmatrix},$$

where

$$A=\frac{1}{\sqrt{2}}\begin{pmatrix}(E_c+1)^{1/2} & (E_c+1)^{1/2}\\ i(E_c-1)^{1/2} & -i(E_c-1)^{1/2}\end{pmatrix}. \tag{29}$$

This yields

$$\left(\frac{d}{dx}-1+\frac{\gamma-i\nu}{x}\right)F_1+\frac{\kappa-i\nu'}{x}F_2 = \frac{1}{2k_c^2}(\delta E-\delta V)(E_cF_1+F_2), \tag{30a}$$

$$\frac{\kappa+i\nu'}{x}F_1+\left(\frac{d}{dx}+\frac{\gamma+i\nu}{x}\right)F_2=\frac{-1}{2k_c^2}(\delta E-\delta V)(F_1+E_cF_2), \tag{30b}$$

where $\nu=aE_c/k_c$, $\nu'=a/k_c=(\nu^2-a^2)^{1/2}$. From (30b) we find

$$F_1(x)=\frac{x}{\kappa+i\nu'}\left\{-\left(\frac{d}{dx}+\frac{\gamma+i\nu}{x}\right)F_2(x) - \frac{1}{2k_c^2}(\delta E-\delta V)[F_1(x)+E_cF_2(x)]\right\}. \tag{31}$$

Substituting the right-hand side of (31) into the left-hand side of (30a) wherever $F_1(x)$ appears, we obtain

$$-x\left[\frac{d^2}{dx^2}+\left(-1+\frac{2\gamma+1}{x}\right)\frac{d}{dx}-\frac{\gamma+i\nu}{x}\right]F_2(x)\equiv\mathfrak{D}_{-i\nu,\gamma}F_2(x) = \frac{\kappa+i\nu'}{2k_c^2}(\delta E-\delta V)[E_cF_1(x)+F_2(x)] + \frac{x}{2k_c^2}\left(\frac{d}{dx}-1+\frac{\gamma-i\nu+1}{x}\right)(\delta E-\delta V)[F_1(x)+E_cF_2(x)]. \tag{32}$$

We now define E_c such that it is given by the expression for the bound-state energy (20) with the substitution $p_c\to ik_c$; that is,

$$\delta E=E-E_c =-\lambda V_1a+\tfrac{1}{2}\lambda^2V_2(E_c\kappa^2+\kappa+3\nu\nu') - \frac{a\lambda^3V_3}{2k_c^2}[(2E_c^2+1)\kappa^2+3E_c\kappa+4\nu^2+\nu'^2-1]. \tag{33}$$

It is evident that δE will be real for real E_c. We note further that the right-hand side of (33) depends on the quantum number κ so that for any given energy E the corresponding value of E_c will be different for each partial wave.

With this choice (33) for the energy shift we see immediately that Eqs. (32) and (33) are identical to the corresponding Eqs. (10) and (11) for the bound state with the substitution $p_c\to ik_c$. Moreover, the boundary condition that the wave function be regular at the origin is the same in each case.[9] It then follows[10] that the continuum solution can be obtained from the bound-state solution with the substitution $p_c\to ik_c$ {which implies also $\eta\to-i\nu$, $\eta'\to-i\nu'$, $\zeta\to-i\xi\equiv\arg[(i\nu-\gamma)/(i\nu'+\kappa)]^{1/2}$}. Hence, we have for the continuum solution

$$F_1(x)=F_1^c(x)+\lambda^2A_2(x)+\lambda^3A_3(x)+\cdots, \qquad F_2(x)=F_2^c(x)+\lambda^2B_2(x)+\lambda^3B_3(x)+\cdots, \tag{34}$$

where the Coulomb functions are given by

$$F_1^c(x)=(\gamma+i\nu)\left(\frac{i\nu-\gamma}{i\nu'+\kappa}\right)^{1/2}M(\gamma+i\nu+1,2\gamma+1,x) =(\gamma+i\nu)e^{ix}M(\gamma+i\nu+1,2\gamma+1,x),$$

$$F_2^c(x)=(\gamma-i\nu)\left(\frac{i\nu+\gamma}{i\nu'-\kappa}\right)^{1/2}M(\gamma+i\nu,2\gamma+1,x) =(\gamma-i\nu)e^{-ix}M(\gamma+i\nu,2\gamma+1,x), \tag{35}$$

and the coefficients $A_n(x)$ and $B_n(x)$ have the form

$$A_n(x)=\sum_{s=-n}^{n}\alpha_s^n(ik_c,\kappa)M(\gamma+i\nu+1-s,2\gamma+1,x),$$

$$B_n(x)=\sum_{s=-n}^{n}\beta_s^n(ik_c,\kappa)M(\gamma+i\nu-s,2\gamma+1,x). \tag{36}$$

In (36), the coefficients $\alpha_s^n(ik_c,\kappa)$ are obtained from Table I by means of the substitution $p_c\to ik_c$, while $\beta_s^n(ik_c,\kappa)$ may be determined by means of the relation

$$\beta_s^n(ik_c,\kappa)=[\alpha_{-s}^n(ik_c,\kappa)]^* \tag{37}$$

which follows from Eq. (19). We note that the screened continuum Dirac wave function is real. This follows from (37) and

$$[e^{-ik_cr}M(\gamma+i\nu-s,2\gamma+1,x)]^* =e^{-ik_cr}M(\gamma+i\nu+1+s,2\gamma+1,x). \tag{38}$$

Although our analytic expansion of the continuum wave function gives a good representation of the exact screened Dirac wave function in the interior region (cf. Figs. 5–8 and Sec. IV), at sufficiently

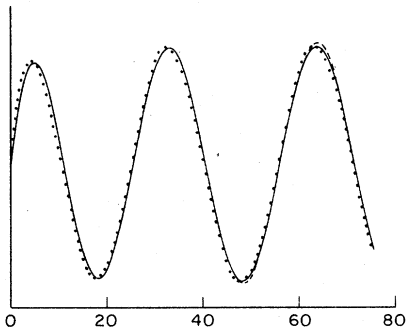

FIG. 5. Upper component (unnormalized) of 10 keV $S_{1/2}$ continuum wave function for aluminum ($Z=13$). The solid curve is the numerical shape obtained for the KS potential, the dashed curve gives our analytic result, and the dotted curve is the point-Coulomb shape for this case. Distances are in electron-Compton wavelengths.

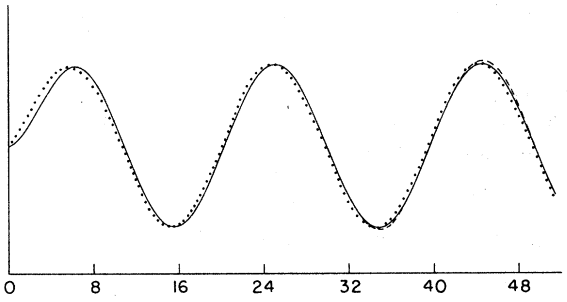

FIG. 7. Upper component (unnormalized) of 25 keV $P_{3/2}$ continuum wave function for zinc ($Z=30$) assuming a Yukawa potential $V(r)=-(a/r)e^{-\lambda r}$, where λ^{-1} is the Thomas-Fermi radius. The unbroken curve is the exact numerical shape, the dashed curve is our analytic result, and the dotted curve the point-Coulomb shape for this case. Distances are in electron-Compton wavelengths.

large distances this approximation breaks down. In order to obtain the continuum normalization, then, we consider the irregular solutions of the Dirac equation. As shown in Ref. 1 this procedure offers a method to extract expansions for the Jost function and hence the continuum normalization.

B. Irregular solutions

As in the nonrelativistic case we will determine the Jost function by decomposing the regular solution as a sum of irregular solutions which are asymptotically either purely incoming or purely outgoing. The coefficients in this expansion can then be identified with the Jost functions.[11]

Let

$$\Psi_\kappa(\pm k,r)=A\begin{pmatrix}\Psi_1(\pm k,r)\\ \Psi_2(\pm k,r)\end{pmatrix}$$

be two linearly independent solutions of Eq. (27) which behave asymptotically as either incoming or outgoing spherical waves. The Jost solutions $f_\kappa(\pm k,r)$ are then defined by the relation

$$f_\kappa(\pm k,r)=r\Psi_\kappa(\pm k,r)\,. \tag{39}$$

Using the normalization we have adopted,[12] the phase of $f_\kappa(\pm k,r)$ is fixed conventionally by the requirement that

$$f_\kappa(\pm k,r)\xrightarrow[r\to\infty]{}\frac{1}{\sqrt{2}}\begin{pmatrix}(E+1)^{1/2}\\ \mp i\,(E-1)^{1/2}\end{pmatrix}e^{\mp ikr}\,. \tag{40}$$

Given the Jost solutions, the Jost functions $f_\kappa(\pm k)$ may be obtained by means of the relation

$$f_\kappa(\pm k)=r^2[\bar{\Psi}_\kappa(\pm k,r)\Phi'_{E\kappa}(r)-\bar{\Psi}'_\kappa(\pm k,r)\Phi_{E\kappa}(r)]\,, \tag{41}$$

where $\Phi_{E\kappa}(r)$ is the regular radial solution and the prime indicates differentiation with respect to r and $\bar{\Psi}=\Psi^+\sigma_z$. It follows from Eqs. (39)–(41) that the regular solution of the Dirac equation can be written in the form

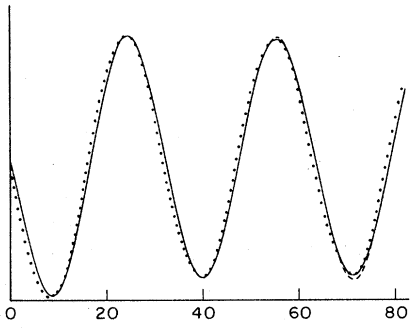

FIG. 6. Lower component (unnormalized) of 10 keV $S_{1/2}$ continuum wave function for Al. Otherwise the same as Fig. 5.

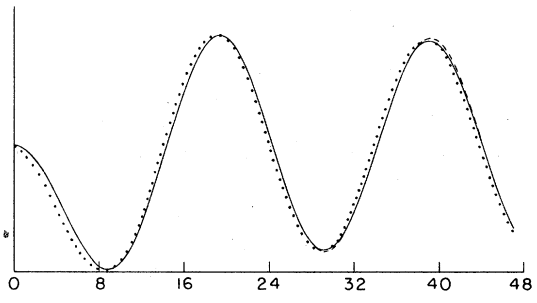

FIG. 8. Lower component (unnormalized) of 25 keV $P_{3/2}$ continuum wave function for Zn. Otherwise the same as Fig. 7.

$$N^{-1}r\Phi_{E\kappa}(r) = (-1/2ik)[f_\kappa(-k)f_\kappa(k,r) - f_\kappa(k)f_\kappa(-k,r)] . \quad (42)$$

For real $k, f_\kappa(-k,r) = f_\kappa^*(k,r)$ and $f_\kappa(-k) = f_\kappa^*(k)$.

It is evident, using (42) and (40), that the continuum normalization is given by

$$N_\kappa(k) = E^{-1/2}\,|f_\kappa(k)\,|^{-1} , \quad (43)$$

while the Dirac phase shift is just

$$\delta_\kappa(k) = \arg f_\kappa(k) + \tfrac{1}{2}\pi l . \quad (44)$$

(l is the angular momentum of the upper component.)

We now assume the screened Jost solution can be written in the form (we omit the angular momentum quantum number for simplicity)

$$f(k,r) = e^{i\phi}(k/k_c)^{1/2}[f_c(k_c,r) + \lambda^2 f_2(k_c,r) + \lambda^3 f_3(k_c,r) + \cdots] , \quad (45)$$

and the corresponding Jost function is given by

$$f(k) = e^{i\phi}(k/k_c)^{1/2}[\,f_c(k_c) + \lambda^2 f_2(k_c) + \lambda^3 f_3(k_c) + \cdots] . \quad (46)$$

The factor $(k/k_c)^{1/2}$ is introduced so that, after substitution into (42), the leading term of the regular solution will be the correct point-Coulomb wave function of shifted energy. The arbitrary phase $\phi(k_c) = -\phi(-k_c)$ allows for the fact that screened and point-Coulomb phase shifts do not coincide in the limit $\lambda \to 0$. Its magnitude must be determined from the asymptotic condition (40). $f_c(k_c,r)$ is the point-Coulomb Jost solution and is given by $f_c(k_c,r) = r\Psi_c(k_c,r)$, where

$$\Psi_c(k_c,r) = A\begin{pmatrix}\psi_1^c(k_c,r)\\ \psi_2^c(k_c,r)\end{pmatrix} \quad (47)$$

and

$$\psi_1^c(k_c,r) = -x^\gamma e^{-x/2}(\gamma+i\nu)e^{2i\xi}e^{-\pi\nu/2} \times \psi(\gamma+i\nu+1, 2\gamma+1, x) ,$$

$$\psi_2^c(k_c,r) = x^\gamma e^{-x/2}e^{-\pi\nu/2}\psi(\gamma+i\nu, 2\gamma+1, x) . \quad (48)$$

In (48), $\psi(a,b,x)$ is an irregular solution of the confluent hypergeometric equation and is discussed in Ref. 1. From this result we find the Coulomb-Jost function,

$$f_c(k_c) = (2ik_c)^{-\gamma+1}e^{-\pi\nu/2}\,\frac{\Gamma(2\gamma+1)}{\Gamma(\gamma+i\nu)}\,e^{i\xi} . \quad (49)$$

Substituting the expressions (45) and (46) into Eq. (42) and separating our expansion of the regular solution into incoming and outgoing parts by means of the identity

$$M(a,b,x) = \frac{\Gamma(b)}{\Gamma(b-a)}\,e^{i\pi a}\psi(a,b,x) + \frac{\Gamma(b)}{\Gamma(a)}\,e^{i\pi(a-b)}e^{x}\psi(b-a,b,-x) , \quad (50)$$

we obtain, after some algebra, an analytic expansion for the screened Dirac-Jost function $f(k_c)$. Defining $f_n(k_c) = f_c(k_c)\chi_n(k_c)$ we find the particular solution for $n = 2, 3$:

$$\chi_n(k_c) = \frac{1}{2}\sum_{s=-n}^{n}(-1)^s\,\frac{\Gamma(\gamma-i\nu)\Gamma(\gamma+i\nu)}{\Gamma(\gamma-i\nu+s)\Gamma(\gamma+i\nu+1-s)} \times e^{-i\xi}\alpha_s^n(ik_c,k) . \quad (51)$$

The corresponding correction to the Jost solution $f_n(k_c,r)$ is given by

$$f_n(k_c,r) = -\chi_n(-k_c)f_c(k_c,r) + A\sum_{s=-n}^{n}\begin{pmatrix} -\dfrac{\Gamma(\gamma-i\nu)}{\Gamma(\gamma-i\nu+s)}\,e^{-\pi\nu/2}(-1)^s e^{i\xi}\alpha_s^n x^\gamma e^{-x/2}\psi(\gamma+i\nu+1-s, 2\gamma+1, x)\\ \dfrac{1}{\gamma-i\nu}\,\dfrac{\Gamma(\gamma-i\nu+1)}{\Gamma(\gamma-i\nu+1+s)}\,e^{-\pi\nu/2}(-1)^s e^{i\xi}\beta_s^n x^\gamma e^{-x/2}\psi(\gamma+i\nu-s, 2\gamma+1, x)\end{pmatrix} . \quad (52)$$

The screened continuum normalization which is found using (46) and (50) in (43) is given by

$$N(k,\kappa) = N_c(k_c,\kappa)(k_cE_c/kE)^{1,2} \times [1 - \lambda^2\,\mathrm{Re}\chi_2(k_c) - \lambda^3\,\mathrm{Re}\chi_3(k_c) - \cdots] , \quad (53)$$

where N_c is the point-Coulomb normalization. This result (52) confirms a conjecture made by Pratt and Tseng[12] based on empirical observations that the product $(kE)^{1/2}N$, compared to the corresponding point-Coulomb quantity of shifted energy, is essentially independent of screening except at very low energy. Thus, our results allow analytic corrections to the normalization screening theory of processes such as photoeffect, etc.

IV. COMPARISON OF ANALYTIC AND NUMERICAL RESULTS

In the preceding sections we have given analytic expressions for screened Dirac radial wave functions, including bound-state energy eigenvalues

and bound and continuum normalizations. In order to assess the accuracy of these expressions we use numerical methods to obtain "exact" results in various relativistic screened potentials. In Figs. 1–8 we have shown comparisons between our analytic results and numerical calculations for the wave-function shapes.

We have made these comparisons primarily for the Yukawa potential $V(r) = -(a/r)e^{-\lambda r}$ and for the self-consistent Kohn-Sham potential (KS), often utilized in relativistic calculations. We will wish to ask how these relativistic results differ from our previous nonrelativistic comparisons. While relativistic and nonrelativistic potentials may differ, this is not true for the usual Yukawa potential; it is true for the self-consistent potentials. The self-consistent potential used here was generated by a modification of the code developed by Liberman *et al.*[13] This potential does reduce to the corresponding nonrelativistic potential in the small Z limit (assuming the same exchange term is used).

We find a similar accuracy of our analytic approximation in both the relativistic and nonrelativistic case assuming the Yukawa potential. We do not find a corresponding result in comparing relativistic Kohn-Sham results with our previously presented nonrelativistic Slater results. This is primarily due to the difference in potentials resulting from the difference in exchange terms. We have verified that similar results are obtained in the relativistic and nonrelativistic cases if the same choice of exchange is made.

The difference between these two self-consistent potentials is to be understood from the fact that at intermediate distances the exchange term is tending to cancel the screening corrections to a point-Coulomb shape. The larger exchange term of the Slater case results in a total potential closer to point Coulomb, for which the perturbation theory converges faster. This effect is particularly pronounced for low Z, where exchange (and correlations also) are most important, and the potential-expansion coefficients V_k are sensitive to the type of exchange term used. This consideration, and the poor convergence of the analytic theory for low Z, are reasons that, if Coulomb predictions are not adequate, one cannot have great confidence in the analytic predictions for low-Z screening corrections.

Although the accuracies of relativistic and nonrelativistic wave functions in the same potential are similar, it is important to realize that the dependence of wave functions on screening is different in the two cases. This can be seen in the analytic theory where, in the relativistic case, there is a term, linear in r, absent in the nonrelativistic case. One sees in the numerical data, Figs. 5–8, large deviations from point-Coulomb shapes at small x which are not present in the nonrelativistic case.

In order to apply our perturbation theory it is necessary to determine the potential coefficients V_k which appear in our expansion of the potential, Eq. (1). For the KS potential we employ a procedure described elsewhere,[4] which requires only a simple least-squares fit to the numerical potential with a polynomial in r of the same order as the order of perturbation theory retained. The range of the fit is chosen to be $0 < r < \lambda^{-1}$, which includes essentially all of the region occupied by the K and L shells, but only part of the higher shells. This procedure for obtaining the V_k, while somewhat unstable with respect to variations in the order or range considered, is considerably simpler than that employed in Ref. 1 and, moreover, yields consistent results for potential coefficients even for highly ionized systems. Typical results for these fits including terms of third order in λ are given in Table II. In the Yukawa case the potential coefficients were obtained from a simple power-series expansion of $V(r)$.

We have made rather extensive comparisons of our analytic expressions for relativistic screened Coulomb wave functions with exact numerical results. We present here a summary of these comparisons for three elements, Al ($Z = 13$), Zn ($Z = 30$), and W ($Z = 74$) which show typical results for low, intermediate, and high Z. For each case data are given for both the Yukawa and KS potentials. For the Yukawa case, somewhat better results for wave functions may be achieved using the same procedure to determine the V_k's as in the KS case.

TABLE II. Potential expansion coefficients from a third-order polynomial least-squares fit to the KS potential with $\lambda = 1.13\ \alpha Z^{1/3}$. We also give values for the Yukawa potential obtained by a Taylor series expansion about $r = 0$.

Z	V_1	V_2	V_3
8	−0.95	0.63	−0.21
13	−1.04	0.74	−0.25
30	−1.13	0.91	−0.35
47	−1.17	0.98	−0.38
50	−1.17	0.99	−0.39
62	−1.19	1.03	−0.41
73	−1.21	1.06	−0.43
74	−1.21	1.06	−0.43
79	−1.23	1.08	−0.44
80	−1.23	1.08	−0.44
82	−1.23	1.09	−0.45
92	−1.24	1.13	−0.47
Yukawa	−1.00	0.50	−0.17

TABLE III. Bound-state wave-function shapes (upper/lower components) for the Yukawa and KS potentials as a function of n, κ, and Z. $R_{max}(\epsilon)$, as defined in the text, is the radial distance at which the relative error ϵ first achieves the specified value. All distances are in electron-Compton wavelengths.

			$R_{max}(\epsilon)$ for Yukawa		$R_{max}(\epsilon)$ for KS		First Bohr	Thomas-Fermi
Z	n	κ	$\epsilon=0.01$ (U/L)	$\epsilon=0.02$ (U/L)	$\epsilon=0.01$ (U/L)	$\epsilon=0.02$ (U/L)	Orbit (a^{-1})	Radius (λ^{-1})
13	1	−1	36/50	43/50	36/50	43/64	10.5	51.6
30	1	−1	27/33	35/41	15/20	22/27	4.6	39.0
	2	−1	24/17	27/22	9/18	31/23		
		1	16/12	21/16	12/9	17/12		
		−2	0/0	27/3	12/32	17/35		
74	1	−1	20/		5/7	8/10	1.8	28.9
	2	−1	16/23	21/27	3/5	13/21		
		1	13/13	19/15	4/3	6/4		
		−2	0/0	26/30	4/9	7/11		

We first consider bound states. In Table III we compare numerical and analytic wave-function shapes for both Yukawa and KS potentials. In order to characterize the results simply we give, as in our nonrelativistic work, the values of the radial distances $R_{max}(\epsilon)$ (in Compton wavelenghts) at which the relative error ϵ of our theoretical shapes compared to the envelope of exact numerical results reaches 1.0% and 2.0% for both upper and lower components (upper/lower). Our data at the 0.1% level is appreciably poorer than in the nonrelativistic case because we have directly used the numerical-potential data rather than a smoothed fit as in our previous work. In Table III we also give values in Compton wavelengths for the first Bohr radius ($=a^{-1}$) and the Thomas-Fermi radius of the atom ($=\lambda^{-1}$). We see that in general our analytic shapes reproduce the numerical results to an accuracy of better than 1% over nearly the entire interior of the atom in the case of inner shells of intermediate- and high-Z elements and for the K shell of all but the lowest-Z elements. The excellent agreement of our analytic wave-function shapes with numerical values explains why we are able to obtain expressions for bound-state normalizations which are also accurate in these

TABLE IV. Relativistic binding energies (in keV) for the Yukawa and KS potentials as a function of n, κ, and Z. For comparisons we also give the point-Coulomb results.

				Binding energies (keV)			Fractional error	
Potential	Z	n	κ	Numerical	Analytic	Coulomb	Analytic	Coulomb
Yukawa	13	1	−1	1.493(0)	1.489	2.305	0.003	0.5
	30	1	−1	9.758(0)	9.758	1.240(1)	0.0	0.3
		2	−1	1.045(0)	9.647(−1)	3.108(0)	0.08	2.0
			1	9.377(−1)	8.740	3.108(0)	0.07	2.3
			−2	9.096(−1)	8.442	3.071(0)	0.07	2.4
	74	1	−1	7.175(1)	7.175	8.091	0.0	0.13
		2	−1	1.254(1)	1.250	2.064	0.003	0.7
			1	1.230(1)	1.226	2.064	0.003	0.7
			−2	1.077(1)	1.073	1.898	0.004	0.8
KS	13	1	−1	1.505(0)	1.503	2.305	0.001	0.5
	30	1	−1	9.506(0)	9.552	1.240(1)	0.005	0.3
		2	−1	1.157(0)	1.099	3.108	0.05	1.7
			1	1.021(0)	9.547(−1)	3.108	0.07	2.0
			−2	9.969(−1)	9.299	3.071(0)	0.07	2.1
	74	1	−1	6.934(1)	7.014	8.911	0.01	0.3
		2	−1	1.196(1)	1.194	2.064	0.002	0.7
			1	1.144(1)	1.146	2.064	0.002	0.8
			−2	1.009(1)	1.005	1.898	0.004	0.9

TABLE V. Bound-state normalizations for the Yukawa and KS potentials as a function of n, κ, and Z. For comparison we also give the point-Coulomb results.

Potential	Z	n	κ	Bound-state normalizations Numerical	Analytic	Coulomb	Fractional error Analytic	Coulomb
Yukawa	13	1	−1	2.885(−2)	2.893	2.963	0.003	0.03
	30	1	−1	1.071(−1)	1.072	1.082	0.0008	0.01
		2	−1	3.435(−2)	3.590	3.888	0.05	0.1
			1	3.282(−2)	3.428	3.888	0.04	0.2
			−2	1.074(−3)	1.047	1.190	0.03	0.1
	74	1	−1	4.840(−1)	4.881	4.894	0.002	0.005
		2	−1	1.842(−1)	1.852	1.911	0.006	0.04
			1	1.822(−1)	1.833	1.911	0.006	0.05
			−2	1.312(−2)	1.240	1.303	0.06	0.007
KS	13	1	−1	2.854(−2)	2.861	2.963	0.002	0.04
	30	1	−1	1.062(−1)	1.065	1.082	0.003	0.02
		2	−1	3.312(−2)	3.431	3.888	0.04	0.2
			1	3.003(−2)	3.113	3.888	0.04	0.3
			−2	9.163(−4)	9.555	1.190(−3)	0.04	0.3
	74	1	−1	4.848(−1)	4.866	4.894	0.004	0.01
		2	−1	1.770(−1)	1.795	1.911	0.01	0.08
			1	1.703(−1)	1.754	1.911	0.03	0.1
			−2	1.143(−2)	1.177	1.303	0.03	0.1

circumstances. These results for shapes go somewhat beyond the work of Pratt and Tseng,[12] so that by using our perturbation theory in the relativistic case we can considerably extend the range of validity of the normalization screening theory.

In Table IV we give our results for atomic binding energies. The difference between analytic and numerical results for the K shell is generally less

TABLE VI. Continuum wave-function shapes (upper/lower components) for the Yukawa and KS potentials as a function of T, the kinetic energy $= E-1$, κ, and Z. $R_{max}(\epsilon)$, as defined in the text, is the radial distance at which the relative error ϵ first achieves the specified value. Distances are in electron-Compton wavelengths.

Z	T(keV)	κ	$R_{max}(\epsilon)$ for Yukawa $\epsilon=0.1$ (U/L)	$\epsilon=0.02$ (U/L)	$R_{max}(\epsilon)$ for KS $\epsilon=0.01$ (U/L)	$\epsilon=0.02$ (U/L)	First Bohr Orbit (a^{-1})	Thomas-Fermi Radius (λ^{-1})	de Broglie Wavelength
13	3	−1	42/35	45/40	23/31	40/34	10.5	51.6	58.0
		1	25/22	29/26	20/17	23/20			
	10	−1	63/58	79/73	47/53	61/69			31.8
		−3	29/36	44/53	23/32	27/35			
		−5	25/37	27/38	21/17	24/25			
	30	−1	75/79	86/90	73/70	84/88			18.3
		−3	47/51	65/69	36/40	46/50			
		6	20/18	22/20	17/16	19/18			
		−7	19/26	22/27	17/25	19/26			
30	30	−1	42/39	45/48	32/29	33/37	4.6	39.0	18.3
		2	25/23	34/31	14/14	23/21			
		−3	25/29	34/31	13/18	23/20			
		−7	15/14	17/25	11/7	13/11			
	100	−1	49/51	58/60	38/40	48/50			
		−3	34/36	44/46	23/26	33/31			
		6	12/11	14/13	10/9	11/10			
		8	12/11	14/12	10/9	11/15			
74	100	−1	21/23	26/28	5/7	20/18	1.8	28.9	10.0
		2	17/16	22/20	5/4	12/15			
		−3	17/15	22/20	5/7	12/14			
		6	10/9	11/10	7/6	8/7			

TABLE VII. Continuum normalizations for the Yukawa and KS potentials as a function of T, the kinetic energy $=E-1$, κ, and Z. For comparison we also give the point-Coulomb results.

Potential	Z	T(keV)	κ	Continuum normalizations			Fractional error	
				Numerical	Analytic	Coulomb	Analytic	Coulomb
Yukawa	13	3	−1	1.190(0)	1.190	1.192	0.000 01	0.002
			1	1.245(0)	1.247	1.912	0.001	0.04
			−2	2.595(−2)	2.598	2.853	0.001	0.1
		10	−1	8.957(−1)	8.956	8.994	0.000 2	0.004
			−3	8.238(−4)	8.240	8.964	0.000 3	0.09
			−5	2.926(−7)	2.881	3.437	0.02	0.2
		30	−1	7.219(−1)	7.218	7.243	0.000 05	0.003
			−3	1.965(−3)	1.965	2.031	0.000 06	0.03
			6	6.001(−8)	5.886	6.199	0.02	0.03
			−7	1.305(−9)	1.279	1.422	0.02	0.09
	30	10	−1	1.397(0)	1.397	1.400	0.000 002	0.002
		30	−1	1.058(0)	1.058	1.062	0.000 007	0.004
			2	7.048(−2)	7.048	7.224	0.000 06	0.03
			−3	3.222(−3)	3.222	3.497	0.000 08	0.09
			−7	1.991(−9)	1.860	2.531	0.07	0.3
		100	−1	7.903(−1)	7.903	7.928	0.000 01	0.03
			−3	7.834(−3)	7.833	8.086	0.000 02	0.03
			6	1.577(−6)	1.565	1.658	0.007	0.05
			−7	6.585(−8)	6.528	7.171	0.009	0.09
	74	50	−1	1.731(0)	1.731	1.739	0.000 04	0.004
		100	−1	1.414(0)	1.414	1.421	0.000 02	0.005
			2	1.985(−1)	1.985	2.046	0.000 01	0.03
			−3	1.767(−2)	1.767	1.921	0.000 06	0.09
			6	3.488(−6)	3.394	4.115	0.03	0.2
KS	13	3	−1	1.191(0)	1.190	1.192	0.001	0.001
			1	1.290(0)	1.295	1.192	0.004	0.08
			−2	2.587(−2)	2.597	2.853	0.004	0.1
		10	−1	8.959(−1)	8.953	8.994	0.000 6	0.004
			−3	8.228(−4)	8.232	8.964	0.000 6	0.09
			4	1.912(−5)	1.849	1.932	0.03	0.01
			−5	2.938(−7)	2.840	3.437	0.03	0.2
		30	−1	7.220(−1)	7.217	7.243	0.000 4	0.003
			−3	1.964(−3)	1.964	2.031	0.000 08	0.03
			6	6.130(−8)	5.885	6.199	0.04	0.01
			−7	1.307(−9)	1.252	1.422	0.04	0.09
	30	10	−1	1.398(0)	1.397	1.400	0.000 4	0.002
		30	−1	1.058(0)	1.058	1.062	0.000 1	0.004
			2	7.088(−2)	7.105	7.224	0.002	0.02
			−3	3.189(−3)	3.196	3.497	0.002	0.1
			−7	1.985(−9)	1.590	2.531	0.2	0.3
		100	−1	7.900(−1)	7.899	7.928	0.000 09	0.004
			−3	7.798(−3)	7.807	8.086	0.001	0.04
			6	1.598(−6)	1.562	1.658	0.02	0.04
			−7	6.547(−8)	6.377	7.171	0.03	0.1
	74	50	−1	1.729(0)	1.731	1.739	0.000 9	0.006
		100	−1	1.412(0)	1.413	1.421	0.001	0.006
			2	1.973(−1)	1.990	2.046	0.001	0.04
			−3	1.726(−2)	1.741	1.921	0.008	0.1
			6	3.630(−6)	3.231	4.115	0.1	0.1

than 1% even for low Z and the agreement tends to become better as Z increases. For the L shell at low Z the relative errors may be quite large. For intermediate and high Z, however, the agreement is generally better than 5% and improves with increasing Z. We also note that the M shell binding energies for W are accurate to within 5–10% although the expected value of the radial distance $\langle r \rangle$ for M-shell electrons is greater than λ^{-1}.

A comparison of our expression for relativistic bound-state normalizations with exact numerical results is given in Table V. The states considered are the same as in Table IV. In general we see that the behavior of the normalization as a function of n, κ, Z, and the potential essentially parallels that of the binding energy so that the same remarks are applicable.

In the continuum case our results are summarized in Tables VI and VII. Again, we consider $Z = 13$, 30, and 74 to cover the range of low to high atomic numbers for both the Yukawa and KS potentials.

In Table VI we give results for continuum shapes with $R_{\max}(\epsilon)$ defined as in the bound-state case. We find that for energies on the order of the K-shell binding energy above threshold, our analytic expression for continuum radial wave-function shape is accurate to better than 1% over the entire interior of the atom and improves with increasing energy. For fixed energy the value of $R_{\max}(\epsilon)$ decreases somewhat as $|\kappa|$ increases. However, even for relatively high angular momenta our results remain very good. It is interesting to note that in the relativistic case the detailed shape of the upper/lower component differs from the corresponding point-Coulomb result. (See Figs. 5–8.) In the nonrelativistic limit these changes combine to give only a phase difference in first approximation. At sufficiently large r near the edge of the atom the amplitude of our analytic expansion begins to deviate significantly from the numerical value. This is due to the fact that the asymptotic behavior of our result is not correct—additional positive powers of r appear in the asymptotic form—and may be traced to the failure of our expansion of the potential at large distances. It is for this reason that we are unable to obtain an analytic expression for the screened phase shift. For reference we also give in Table VI the values in Compton wavelengths of the Bohr radius (a^{-1}), the Thomas-Fermi radius of the atom (λ^{-1}), and the de Broglie wavelength of the electron (k^{-1}).

Finally, in Table VII we compare continuum normalizations in our theory with exact numerical results and with the corresponding point-Coulomb values for the same Z. At energies on the order of the K-shell binding energy above threshold and higher and for $|\kappa| < 8$, we find that our results in general are accurate to better than 1% and improve with increasing energy. For a given element at fixed energy, the accuracy of our results decreases as $|\kappa|$ increases. Even for these higher partial waves, however, we see that our analytic expression for the relativistic screened continuum normalization represents a considerable improvement over the point-Coulomb values.

APPENDIX

For many applications of our theory it may be convenient to employ analytic continuum wave functions in which the energy shift $\delta E = E - E_c$ is, initially, essentially arbitrary. In this way the final choice of δE may be determined by the physical situation. In the following we will indicate the modifications which are necessary in the relativistic case to accomodate this additional degree of freedom. The argument parallels that of Ref. 2 so that only the final results are given here.

We will assume as in Ref. 2 that $E_1 = -V_1 a_1$ since in this case the first-order correction to the wave function vanishes. For most applications of our theory this is the correct physical choice. The method can, of course, be generalized to arbitrary E_1 but the resulting expression for the wave function will be considerably more complicated. In this case we have

$$E - E_c = -V_1 \lambda a + \lambda^2 E_2 + \lambda^3 E_3 + \cdots , \tag{A1}$$

where the E_k are now arbitrary. We find that the screened radial functions $F_1(x)$ and $F_2(x)$ again have the form

$$\begin{aligned} F_1(x) &= F_1^c(x) + \lambda^2 A_2(x) + \lambda^3 A_3(x) + \cdots , \\ F_2(x) &= F_2^c(x) + \lambda^2 B_2(x) + \lambda^3 B_3(x) + \cdots , \end{aligned} \tag{A2}$$

where $F_1^c(x)$ and $F_2^c(x)$ are the point-Coulomb solutions of shifted energy E_c. The coefficients A_n and B_n, however, now have the form

$$\begin{aligned} A_n(x) &= \sum_{s=-n}^{n} \bar{\alpha}_s^n(ik_c, \kappa) M(\gamma + i\nu + 1 - s,\ 2\gamma + 1, x) \\ &\quad + a_0^n(ik_c, \kappa)\ \frac{\partial}{\partial(i\nu)}\ M(\gamma + i\nu + 1, 2\gamma + 1, x) , \\ B_n(x) &= \sum_{s=-n}^{n} \bar{\beta}_s^n(ik_c, \kappa) M(\gamma + i\nu - s,\ 2\gamma + 1, x) \\ &\quad + b_0^n(ik_c, \kappa)\ \frac{\partial}{\partial(i\nu)}\ M(\gamma + i\nu, 2\gamma + 1, x) . \end{aligned} \tag{A3}$$

In (A3), the coefficients $\bar{\beta}_s^n, b_0^n$ are given in terms of the $\bar{\alpha}_s^n$, a_0^n by means of the relations

$$\bar{\beta}_s^n(ik_c, \kappa) = [\bar{\alpha}_{-s}^n(ik_c, \kappa)]^* \tag{A4}$$

TABLE VIII. The independent a_0^n and $\bar{\alpha}_s^n$.

$$a_0^2=(V_2/2k_c^2)i\nu'(\gamma+i\nu)e^{i\xi}(E_c\kappa^2+\kappa+3\nu\nu'-2d_2),\quad d_2=E_2/V_2.$$

$$\bar{\alpha}_{-1}^2=(V_2/2k_c^2)(\gamma+i\nu)(\gamma+i\nu+1)e^{i\xi}\{d_2E_c+i\nu'[i\nu'+E_c(1+i\nu)]\},$$

$$\bar{\alpha}_{+1}^2=-(V_2/4k_c^2)(\gamma-i\nu)e^{-i\xi}\{[E_c(\kappa-i\nu')+1][2d_2-i\nu'(1-2i\nu)]$$
$$+i\nu'(\gamma-i\nu+1)(\gamma+i\nu-1)+i\nu'(\gamma+i\nu)e^{2i\xi}[\kappa-i\nu'+E_c]\},$$

$$\bar{\alpha}_0^2=-\sum_{s=-2}^{2}{}'\,\bar{\alpha}_s^2=-(\bar{\alpha}_{-2}^2+\bar{\alpha}_{-1}^2+\bar{\alpha}_{+1}^2+\bar{\alpha}_{+2}^2).$$

$$a_0^3=-(aV_3/2k_c^4)i\nu'(\gamma+i\nu)e^{i\xi}[d_3+(2E_c^2+1)\kappa^2+3E_c\kappa+4\nu^2+\nu'^2-1],\quad d_3=2k_c^2E_3/aV_3,$$

$$\bar{\alpha}_{-1}^3=(aV_3/8k_c^4)(\gamma+i\nu)(\gamma+i\nu+1)e^{i\xi}[E_c(2d_3+3\gamma^2+7\nu^2-\nu'^2$$
$$-10i\nu-6)+3\kappa-5i\nu'+9\nu\nu'],$$

$$\bar{\alpha}_{+1}^3=-(aV_3/8k_c^4)(\gamma-i\nu)e^{-i\xi}\{[E_c(\kappa-i\nu')+1][2d_3+(\gamma-i\nu+1)(\gamma+i\nu-1)-(2i\nu-1)^2+(\gamma^2+\nu^2)]$$
$$-(\gamma+i\nu-1)(\gamma+i\nu+1)[4i\nu-4-E_c(\kappa-i\nu')]$$
$$-4i\nu(\gamma+i\nu)e^{2i\xi}[E_c+\kappa-i\nu']\},$$

$$\bar{\alpha}_0^3=-\sum_{s=-3}^{3}{}'\,\bar{\alpha}_s^3=-(\bar{\alpha}_{-3}^3+\bar{\alpha}_{-2}^3+\bar{\alpha}_{-1}^3+\bar{\alpha}_{+1}^3+\bar{\alpha}_{+2}^3+\bar{\alpha}_{+3}^3).$$

and

$$b_0^n(ik_c,\kappa)=-[a_0^n(ik_c,\kappa)]^*\ . \tag{A5}$$

We also have, for $|s|>1$,

$$\bar{\alpha}_s^n(ik_c,\kappa)=\alpha_s^n(ik_c,\kappa)\ , \tag{A6}$$

where the α_s^n have the same form as those determined from Table I. Explicit values of the independent $\bar{\alpha}_s^n$ and a_0^n are given in Table VIII.

By considering the irregular solution we also obtain an expression for the Jost function for arbitrary energy shift. If we write, as before,

$$f(k)=e^{i\phi}(k/k_c)^{1/2}f_c(k_c)$$
$$\times[1+\lambda^2\chi_2(k_c)+\lambda^3\chi_3(k_c)+\cdots]\ , \tag{A7}$$

then we find the particular solutions for $n=2,3$:

$$\chi_n(k_c)=\frac{1}{2}\sum_{s=-n}^{n}(-1)^s\,\frac{\Gamma(\gamma-i\nu)\Gamma(\gamma+i\nu)}{\Gamma(\gamma-i\nu+s)\Gamma(\gamma+i\nu+1-s)}$$
$$\times e^{-i\xi}\bar{\alpha}_s^n(ik_c,\kappa)+\frac{1}{2}\,e^{-i\xi}a_0^n(ik_c,\kappa)$$
$$\times|\Gamma(\gamma+i\nu)|^2e^{\pi\nu}\,\frac{\partial}{\partial(i\nu)}$$
$$\times\frac{e^{-\pi\nu}}{(\gamma+i\nu)\,|\Gamma(\gamma+i\nu)|^2}\ . \tag{A8}$$

*Work supported by NSF Grant Nos. PHY74-03531 A03 and OIP-7202883.

†Present address: 14112 Castle Boulevard, Apartment 103, Silver Spring, Md. 20904.

[1]James McEnnan, Lynn Kissel, and R. H. Pratt, Phys. Rev. A 13, 532 (1976); 13, 2325 (E) (1976).

[2]James McEnnan, Lynn Kissel, and R. H. Pratt, Phys. Rev. A 14, 521 (1976).

[3]Sung Dahm Oh, James McEnnan, and R. H. Pratt, Phys. Rev. A 14, 1428 (1976).

[4]James McEnnan, David J. Botto, and R. H. Pratt (to be published).

[5]D. Bunaciu and V. Florescu, Rev. Roum. Phys. 22, 157 (1977).

[6]Zbigniew Iwinski and R. H. Pratt (unpublished).

[7]We are also extending the formalism to include the full continuum wave function and work is in progress on a calculation of the screening corrections to the bremsstrahlung total cross section. See Adam Bechler, Zbigniew Iwinski, and R. H. Pratt (unpublished).

[8]See Ref. 1 for a discussion of the reason why the first-order terms may be omitted in the expansion of the wave function.

[9]The *boundary* condition on the wave function in both the bound and continuum case is that the wave function be regular at the origin. In addition, for bound states the energy must be an eigenvalue so that the wave function will be square integrable.

[10]Theorem of Poincaré: If a differential equation depends holomorphically on a parameter and the boundary conditions are independent of that parameter, then the solutions of the equation are holomorphic functions of the parameter.

[11]In the relativistic case the Jost function should really be represented as a 2×2 matrix due to the spin of the electron. However, since this matrix is proportional to the identity matrix we can simply characterize it as a scalar function.

[12]R. H. Pratt and H. K. Tseng, Phys. Rev. A 5, 1065 (1972).

[13]D. Liberman, J. T. Waber, and Don T. Cromer, Phys. Rev. 137, A27 (1965).